

C.2a.1.8-
Lesbani_2018_IOP_Conf._Ser._Mater._S
ci._Eng._299_012084.pdf

By Risfidian Mohadi

PAPER • OPEN ACCESS

Metal Oxide Supported Vanadium Substituted Keggin Type Polyoxometalates as Catalyst For Oxidation of Dibenzothiophene

To cite this article: Aldes Lesbani *et al* 2018 *IOP Conf. Ser.: Mater. Sci. Eng.* **299** 012084

2
View the [article online](#) for updates and enhancements.

You may also like

- 7** [nanodiamonds carrying silicon-vacancy quantum emitters with almost lifetime-limited linewidths](#)
Uwe Jantzen, Andrea B Kurz, Daniel S Rudnicki *et al.*
- 5** [Synthesis of SiV-diamond particulates via the microwave plasma chemical deposition](#)
- 5** [Ultrananocrystalline diamond on soda-lime glass fibers](#)
Srinivasu Kunuku, Yen-Chun Chen, Chien-Jui Yeh *et al.*
- [The Surface Effect on the Growth of Related Color Centers in Diam](#)
Yu Guo, Zhuan Li, Yang Wang *et al.*

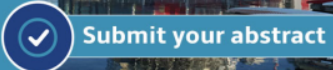


ECS The Electrochemical Society
Advancing solid state & electrochemical science & technology

241st ECS Meeting

May 29 – June 2, 2022 Vancouver • BC • Canada
Abstract submission deadline: **Dec 3, 2021**

Connect. Engage. Champion. Empower. Accelerate.
We move science forward

 Submit your abstract

This content was downloaded from IP address 125.167.57.2 on 26/11/2021 at 14:40

Metal Oxide Supported Vanadium Substituted Keggin Type Polyoxometalates as Catalyst For Oxidation of Dibenzothiophene

Aldes Lesbani*, Sarah Novri Meilyana, Nofi Karim, Nurlisa Hidayati,
Muhammad Said, Risfidian Mohadi, Miksusanti

Department of Chemistry, Faculty of Mathematic and Natural Sciences, Sriwijaya
University, Sumatera Selatan, Indonesia

*e-mail : aldeslesbani@pps.unsri.ac.id

Abstract. Supported polyoxometalate $H_4[\gamma-H_2SiV_2W_{10}O_{40}] \cdot nH_2O$ with metal oxide *i.e.* silica, titanium, and tantalum was successfully synthesized via wet impregnation method to form $H_4[\gamma-H_2SiV_2W_{10}O_{40}] \cdot nH_2O-Si$, $H_4[\gamma-H_2SiV_2W_{10}O_{40}] \cdot nH_2O-Ti$, and $H_4[\gamma-H_2SiV_2W_{10}O_{40}] \cdot nH_2O-Ta$. Characterization was performed using FTIR spectroscopy, X-Ray analyses, and morphology analyses using SEM. All compounds were used as the catalyst for desulfurization of dibenzothiophene (DBT). Silica and titanium supported polyoxometalate $H_4[\gamma-H_2SiV_2W_{10}O_{40}] \cdot nH_2O$ better than tantalum due to retaining crystallinity after impregnation process. On the other hand, compound $H_4[\gamma-H_2SiV_2W_{10}O_{40}] \cdot nH_2O-Ta$ showed high catalytic activity than other supported metal oxides for desulfurization of DBT. Optimization desulfurization process resulted in 99% conversion of DBT under a mild condition at 70 °C, 0.1 g catalyst, and reaction for 3 hours. Regeneration studies showed catalyst $H_4[\gamma-H_2SiV_2W_{10}O_{40}] \cdot nH_2O-Ti$ was remaining catalytic activity for desulfurization of DBT. Keywords: vanadium, Keggin type polyoxometalate, metal oxide, dibenzothiophene

1. Introduction

Fossil fuel naturally contains organic and inorganic compounds [1]. Inorganic element such as sulfur in fossil fuel caused environmental problems [2]. Therefore, clean fossil fuel without sulfur is crucial to keep green environment. The conventional process to remove sulfur from fossil fuel using hydrodesulfurization (HDS) [3]. In this process, sulfides, disulfides, and thiols were successfully removed but organocompounds such as benzothiophene, dibenzothiophene and its derivatives with the high refractory index cannot be reduced [4]. Thus, other methods are needed for the removal of organosulfur.

Recent technology to remove organosulfur has been developed such as oxidative desulfurization (OD) under mild conditions [5-6]. In OD method, organosulfur with high steric hindrance is converted to the corresponding polar sulfone which can be easily removed by extraction or by adsorption. The successful key for OD is a catalyst which is important for activation of a green oxidant such as hydrogen peroxide [7]. Hydrogen peroxide is extensively used as oxidant due to produce water as a by-product after catalytic process [8].



Various catalysts have been tested for OD process such as ionic liquid [9], mesoporous silica [10], transition metal complex [11], tungsten supported on resin [12], tungsten and molybdenum based catalysts such as polyoxometalate compounds [13]. Polyoxometalates are early transition metal-oxygen cluster with various structures, oxidation states, and acidity level [14-15]. These compounds were intensively used as a catalyst for organic synthesis and transformation including OD process. Polyoxometalates [16], peroxometallate [17], supported polyoxometalate [18], and also polyoxometalate nanocomposites [19] were applied as a catalyst for OD process with moderate to excellent yield under mild conditions. Lesbani *et.al.* also used metal oxides supported polyoxometalate as a catalyst for OD of benzothiophene with high yield conversion under mild conditions using hydrogen peroxide as oxidant [20].

Herein, polyoxometalate $H_4[\gamma-H_2SiV_2W_{10}O_{40}] \cdot nH_2O$ was supported with various metal oxides such as silica, titanium, and tantalum to know the efficiency and catalytic activity of supported various metal oxides on polyoxometalate for OD of DBT. Several factors such as catalyst weight, temperature, reaction time, and also the regeneration of catalyst were investigated systematically to obtain high conversion of DBT into the corresponding sulfone as shown in Figure 1.

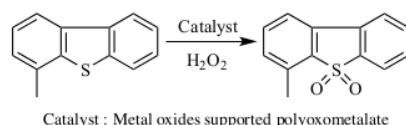


Figure 1. Oxidative desulfurization of DBT into corresponding sulfone.

2. Materials and Methodology

2.1. Chemical

Chemical reagents were purchased from Merck and Sigma-Aldrich such as dibenzothiophene (Sigma-Aldrich), sodium tungsten (Merck), titanium oxide (Merck), tantalum(V) chloride (Sigma-Aldrich), silicon dioxide (Merck), sodium metavanadate (Aldrich), hydrochloric acid (Merck), potassium chloride (Merck), diethyl ether (Merck), potassium carbonate (Merck), acetone (Sigma-Aldrich), ethanol (Merck), methanol (Merck), hydrogen peroxide (Merck), and ammonia (Merck).

2.2. Instrumentation

FTIR analysis was conducted using FTIR Shimadzu Prestige-21 spectrophotometer with KBr disc, and the sample was analyzed in the range of 300-4000 cm^{-1} . XRD powder analysis was performed using XRD Shimadzu LabX type-6000. Sample was scanning at $1^\circ \cdot min^{-1}$. Morphology was analyzed using Jeol JED-2300 SEM analysis station. Catalytic reaction was monitored using Shimadzu GC 2010 Plus equipped with the RTX-1 capillary column.

2.3. Synthesis of $H_4[\gamma-H_2SiV_2W_{10}O_{40}] \cdot nH_2O$ and Characterization [21]

Compound $H_4[\gamma-H_2SiV_2W_{10}O_{40}] \cdot nH_2O$ was synthesis from $Rb_2K_2[\gamma-SiV_2W_{10}O_{40}] \cdot nH_2O$ [22] by extraction as follow: 5 g of $Rb_2K_2[\gamma-SiV_2W_{10}O_{40}] \cdot nH_2O$ was dissolved in 20 mL HCl 1 M, and the solution was transferred to a separatory funnel. Diethyl ether (10 mL) was added slowly into funnel followed by addition of a cold mixture of 15 mL diethyl ether and 15 mL concentrated HCl. The solution was mixed slowly. The heaviest layer was collected, and diethyl ether layer was removed under vacuum. The yellow solid was dissolved in minimum amount of water and solution was a vacuum to produce $H_4[\gamma-H_2SiV_2W_{10}O_{40}] \cdot nH_2O$. Characterization of $H_4[\gamma-H_2SiV_2W_{10}O_{40}] \cdot nH_2O$ was carried out using FTIR spectroscopy, XRD and SEM analyses.

2.4. Preparation of $H_4[\gamma-H_2SiV_2W_{10}O_{40}] \cdot nH_2O$ -Metal Oxides and Characterization

a. $H_4[\gamma-H_2SiV_2W_{10}O_{40}] \cdot nH_2O$ -Si [23]

Preparation of $H_4[\gamma-H_2SiV_2W_{10}O_{40}] \cdot nH_2O$ -Si was adopted from Newman *et.al* (2006) with slight modification was followed: 1 g of $H_4[\gamma-H_2SiV_2W_{10}O_{40}] \cdot nH_2O$ was dissolved with 50 mL methanol in 100 mL Beaker glass equipped with magnetic stirring. To the solution, 25 g of SiO_2 was added slowly, and the mixtures were stirred at medium speed for one h. The mixtures were kept overnight, and volume of solvent was reduced under vacuum to form $H_4[\gamma-H_2SiV_2W_{10}O_{40}] \cdot nH_2O$ -Si, which was washed with acetone several times.

b. $H_4[\gamma-H_2SiV_2W_{10}O_{40}] \cdot nH_2O$ -Ti [24]

Compound $H_4[\gamma-H_2SiV_2W_{10}O_{40}] \cdot nH_2O$ -Ti was prepared as follow: 1 g of titanium oxide was mixed with 25 mL of ethanol. During stirring process, 1 g of $H_4[\gamma-H_2SiV_2W_{10}O_{40}] \cdot nH_2O$ was added. The reaction mixtures were heated at 60 °C for 30 min. The solid was washed with acetone and dried under vacuum to produce $H_4[\gamma-H_2SiV_2W_{10}O_{40}] \cdot nH_2O$ -Ti.

c. $H_4[\gamma-H_2SiV_2W_{10}O_{40}] \cdot nH_2O$ -Ta [25]

Compound $H_4[\gamma-H_2SiV_2W_{10}O_{40}] \cdot nH_2O$ -Ta was prepared by a sol-gel method according to Leilei *et. al.* [25] as follow: 0.5 g of $H_4[\gamma-H_2SiV_2W_{10}O_{40}] \cdot nH_2O$ was dissolved with five mL of ethanol and two mL of water (solution A). Tantalum(V) chloride (0.6 g) was dissolve with 5 mL of ethanol (solution B). Solution A was mixed with solution B with stirring for one h until homogeneous sol formed. The homogeneous sol was kept overnight at 40 °C. Sol was heated at 150 °C for 3 h to form $H_4[\gamma-H_2SiV_2W_{10}O_{40}] \cdot nH_2O$ -Ta. The solid was washed with ethanol and water until the filtrate was neutral. Characterization of $H_4[\gamma-H_2SiV_2W_{10}O_{40}] \cdot nH_2O$ -metal oxides was conducted using FTIR, XRD, and SEM analyses.

2.5. Catalytic Oxidation of Dibenzothiophene [26]

Oxidation of dibenzothiophene was conducted using 250 mL Schlenk flask under oxygen atmospheric condition equipped with a magnetic bar and hot plate. In the flask, 0.1 g of catalyst, 0.1 g of dibenzothiophene, five mL of hexane, and 0.5 mL hydrogen peroxide were added slowly. The reaction mixtures were stirred for several hours and formation of sulfone was detected using GC at various times. Conversion of dibenzothiophene to sulfone was calculated by comparison chromatogram area of dibenzothiophene after reaction at the definite time and initial time. Oxidation of dibenzothiophene was studied through the selection of catalysts, reaction times, a weight of catalysts, and temperature reaction.

3. Result and Discussion

3.1. Preparation of Catalyst

The FTIR spectrum of the synthesized materials is shown in Figure 2. Vanadium substituted Keggin type polyoxometalate $H_4[\gamma-H_2SiV_2W_{10}O_{40}] \cdot nH_2O$ has typical IR bands at 972 cm^{-1} (band for W=O in the exterior of WO_6), 910 cm^{-1} (band for Si-O), 864 cm^{-1} and 779 cm^{-1} (bands for the W-Ob-W, and W-Oc-W, respectively) [27]. The peaks of polyoxometalate-metal oxides as shown in Figure 2 for $H_4[\gamma-H_2SiV_2W_{10}O_{40}] \cdot nH_2O$ -Si (B) $H_4[\gamma-H_2SiV_2W_{10}O_{40}] \cdot nH_2O$ -Ti (C), and $H_4[\gamma-H_2SiV_2W_{10}O_{40}] \cdot nH_2O$ -Ta (D) has a unique vibration for each material due to metal oxides. The main peaks of $H_4[\gamma-H_2SiV_2W_{10}O_{40}] \cdot nH_2O$ after dispersion with metal oxides almost was shifted to the lower wavelength. $H_4[\gamma-H_2SiV_2W_{10}O_{40}] \cdot nH_2O$ -Si has a vibration at 964 cm^{-1} , 910 cm^{-1} , and 779 cm^{-1} for Keggin type and 1088 cm^{-1} and 1381 cm^{-1} for additional peaks related with strong interaction between silica and polyoxometalate. The vibration of polyoxometalate $H_4[\gamma-H_2SiV_2W_{10}O_{40}] \cdot nH_2O$ in $H_4[\gamma-H_2SiV_2W_{10}O_{40}] \cdot nH_2O$ -Si almost low and to be disappeared. Similar phenomena were found for vibration of $H_4[\gamma-H_2SiV_2W_{10}O_{40}] \cdot nH_2O$ -Ti in Figure 2 C where metal oxide was dominant after the interaction. The use of tantalum as metal supported polyoxometalate gave board vibration of $H_4[\gamma$

$\text{H}_2\text{SiV}_2\text{W}_{10}\text{O}_{40}\cdot n\text{H}_2\text{O}\text{-Ta}$ at $670\text{-}780\text{ cm}^{-1}$ as shown in Figure 2D attributed to the dispersion of tantalum into W-Ob-W and W-Oc-W in the both interior and exterior of polyoxometalate cage.

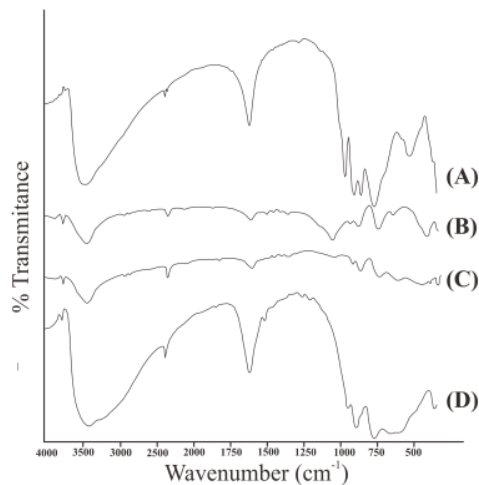


Figure 2. FTIR spectrum of $\text{H}_4[\gamma\text{-H}_2\text{SiV}_2\text{W}_{10}\text{O}_{40}]\cdot n\text{H}_2\text{O}$ (A) and $\text{H}_4[\gamma\text{-H}_2\text{SiV}_2\text{W}_{10}\text{O}_{40}]\cdot n\text{H}_2\text{O}\text{-Si}$ (B), $\text{H}_4[\gamma\text{-H}_2\text{SiV}_2\text{W}_{10}\text{O}_{40}]\cdot n\text{H}_2\text{O}\text{-Ti}$ (C), and $\text{H}_4[\gamma\text{-H}_2\text{SiV}_2\text{W}_{10}\text{O}_{40}]\cdot n\text{H}_2\text{O}\text{-Ta}$ (D)

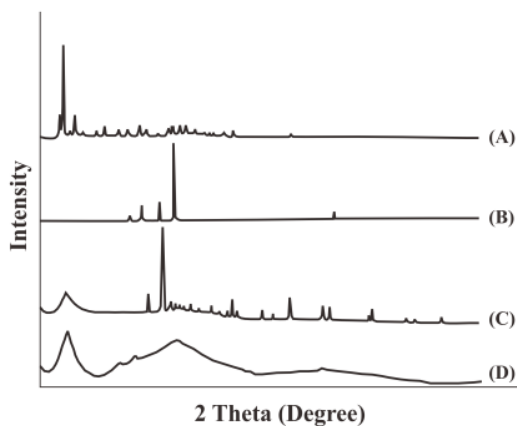


Figure 3. XRD Powder patterns of $\text{H}_4[\gamma\text{-H}_2\text{SiV}_2\text{W}_{10}\text{O}_{40}]\cdot n\text{H}_2\text{O}$ (A) and $\text{H}_4[\gamma\text{-H}_2\text{SiV}_2\text{W}_{10}\text{O}_{40}]\cdot n\text{H}_2\text{O}\text{-Si}$ (B), $\text{H}_4[\gamma\text{-H}_2\text{SiV}_2\text{W}_{10}\text{O}_{40}]\cdot n\text{H}_2\text{O}\text{-Ti}$ (C), and $\text{H}_4[\gamma\text{-H}_2\text{SiV}_2\text{W}_{10}\text{O}_{40}]\cdot n\text{H}_2\text{O}\text{-Ta}$ (D).

Figure 3 shows XRD powder patterns of $\text{H}_4[\gamma\text{-H}_2\text{SiV}_2\text{W}_{10}\text{O}_{40}]\cdot n\text{H}_2\text{O}$ (A) and $\text{H}_4[\gamma\text{-H}_2\text{SiV}_2\text{W}_{10}\text{O}_{40}]\cdot n\text{H}_2\text{O}\text{-Si}$ (B), $\text{H}_4[\gamma\text{-H}_2\text{SiV}_2\text{W}_{10}\text{O}_{40}]\cdot n\text{H}_2\text{O}\text{-Ti}$ (C), and $\text{H}_4[\gamma\text{-H}_2\text{SiV}_2\text{W}_{10}\text{O}_{40}]\cdot n\text{H}_2\text{O}\text{-Ta}$ (D). Crystalline polyoxometalate $\text{H}_4[\gamma\text{-H}_2\text{SiV}_2\text{W}_{10}\text{O}_{40}]\cdot n\text{H}_2\text{O}$ was observed in Figure 3a. On the other hand, although crystallinity of $\text{H}_4[\gamma\text{-H}_2\text{SiV}_2\text{W}_{10}\text{O}_{40}]\cdot n\text{H}_2\text{O}\text{-Si}$ still retain, diffraction peaks of polyoxometalate at 2θ of 3-8 deg was lost. Probably the main Keggin structure was collapsed due to the strong effect of silica to exchange the heteroatom. The balancing effect between polyoxometalate

and metal oxides was appeared on $H_4[\gamma-H_2SiV_2W_{10}O_{40}] \cdot nH_2O$ -Ti and $H_4[\gamma-H_2SiV_2W_{10}O_{40}] \cdot nH_2O$ -Ta as shown in Figure 3 C and D, respectively. In that case, diffraction of polyoxometalate at 2θ of 3-8 deg was broad, and vibration of metal oxide appeared at 2θ of 20-30 deg. Titanium and tantalum gave low exchange effect compare with silica to change heteroatom in Keggin structure.

The morphology of metal oxides supported vanadium substituted Keggin type polyoxometalate $H_4[\gamma-H_2SiV_2W_{10}O_{40}] \cdot nH_2O$ were shown in Figure 4A-D. SEM images indicated block irregular shape of $H_4[\gamma-H_2SiV_2W_{10}O_{40}] \cdot nH_2O$. SEM images of metal oxides supported $H_4[\gamma-H_2SiV_2W_{10}O_{40}] \cdot nH_2O$ were different with original polyoxometalate with the size of images in the range of 220-830 nm while polyoxometalate has 5.2 μm . As an application of materials for OD catalyst, small, regular shape and low size of materials is appropriate due to large contact interaction between substrate and catalyst.

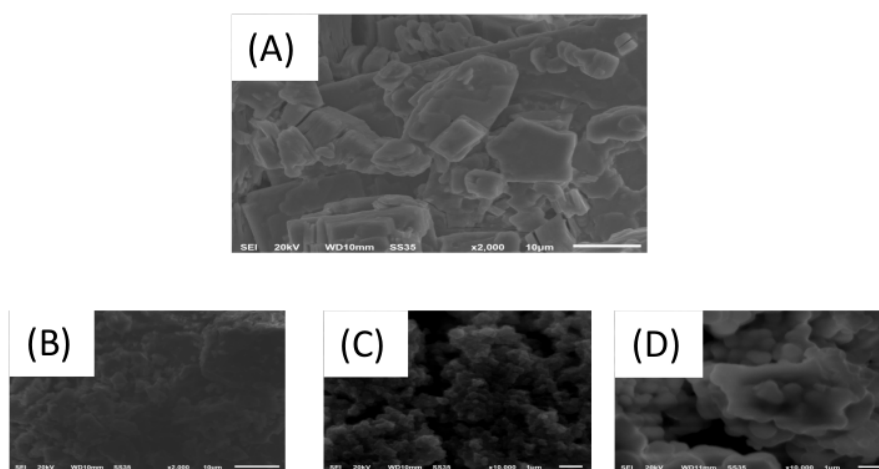


Figure 4. Morphology of $H_4[\gamma-H_2SiV_2W_{10}O_{40}] \cdot nH_2O$ (A) and $H_4[\gamma-H_2SiV_2W_{10}O_{40}] \cdot nH_2O$ -Si (B), $H_4[\gamma-H_2SiV_2W_{10}O_{40}] \cdot nH_2O$ -Ti (C), and $H_4[\gamma-H_2SiV_2W_{10}O_{40}] \cdot nH_2O$ -Ta (D).

9 3.2. Catalytic Activity

3.2.1. Effect of Various Metal Oxide

The effect of metal oxides on the conversion of DBT was evaluated to know the role of metal supported polyoxometalate as a catalyst. The results are shown in Table 1. Tantalum supported Keggin type polyoxometalate $H_4[\gamma-H_2SiV_2W_{10}O_{40}] \cdot nH_2O$ has higher catalytic activity than other metal oxides supported polyoxometalate at reaction time 3 h. This result was similar with OD of dibenzothiophene using tantalum supported Dawson type polyoxometalate $(NH_4)_6[\beta-P_2W_{18}O_{62}] \cdot nH_2O$ -Ta as a catalyst [28]. Original polyoxometalate $H_4[\gamma-H_2SiV_2W_{10}O_{40}] \cdot nH_2O$ shows lower catalytic activity than metal oxides supported polyoxometalate. Thus metal oxides supported polyoxometalate gave an effect into the addition of catalytic activity of desulfurization of DBT. The effect of catalytic activity depended on kinds of metal oxides as support materials.

Table 1. Oxidation of Dibenzothiophene Using Various Catalysts

No	Catalyst	% Conversion
1	$H_4[\gamma-H_2SiV_2W_{10}O_{40}] \cdot nH_2O$	31.50
2	$H_4[\gamma-H_2SiV_2W_{10}O_{40}] \cdot nH_2O -Si$	41.40
3	$H_4[\gamma-H_2SiV_2W_{10}O_{40}] \cdot nH_2O -Ta$	56.60
4	$H_4[\gamma-H_2SiV_2W_{10}O_{40}] \cdot nH_2O -Ti$	38.10

3.2.2. Effect of Catalyst Weight

Desulfurization of dibenzothiophene was conducted systematically using catalyst $H_4[\gamma-H_2SiV_2W_{10}O_{40}] \cdot nH_2O-Ta$. In the first experiment, the effect of catalyst weight was investigated, and the results are shown in Figure 5.

When the catalyst weight was increased from 0.01 to 0.05, the conversion of dibenzothiophene was increased from 19% to 32%. Further increase of the weight of the catalyst to 0.1 g led to 58.5% of dibenzothiophene conversion. On the other hand, the conversion of dibenzothiophene was sharply decreased to 36% when 0.15 g catalyst was used. Therefore, the catalyst weight of 0.1 g was preferable for oxidation of dibenzothiophene. Similar results was found for desulfurization of dibenzothiophene using $(NH_4)[\beta-P_2W_{18}O_{62}]/Ta$ as catalyst [28].

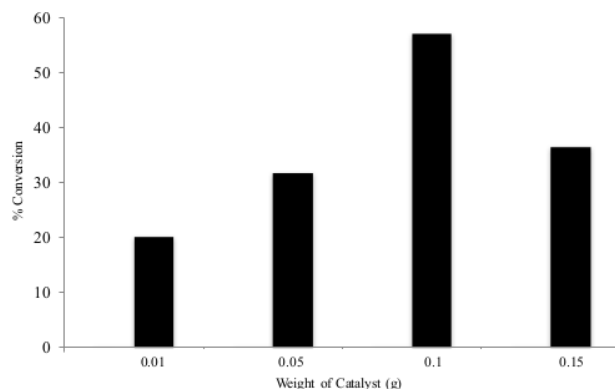


Figure 5. Effect of Catalyst Weight in the Oxidation of Dibenzothiophene Using $H_4[\gamma-H_2SiV_2W_{10}O_{40}] \cdot nH_2O-Ta$

3.2.3. Effect of Temperature

Temperature oxidation is an important parameter for oxidation of dibenzothiophene. In this research, the effect of temperature on oxidation of dibenzothiophene was conducted at mild conditions ranging from 30 – 75 °C as shown in Figure 6. Oxidation of dibenzothiophene was slowly increased from 30 – 50 °C and dramatically changed from 50 – 70 °C. The conversion of dibenzothiophene reached up to 60% at 70 °C and did not change with increasing temperature to 75 °C. Thus oxidation of

dibenzothiophene was successfully conducted at mild conditions using catalyst $H_4[\gamma-H_2SiV_2W_{10}O_{40}] \cdot nH_2O-Ta$.

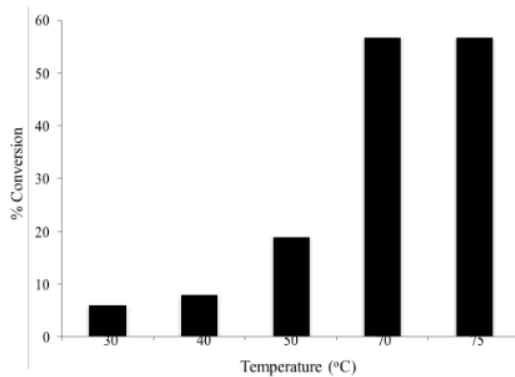


Figure 6. Effect of Temperature in the Oxidation of Dibenzothiophene Using $H_4[\gamma-H_2SiV_2W_{10}O_{40}] \cdot nH_2O-Ta$

3.2.4. Effect of Reaction Time

Desulfurization process of dibenzothiophene was continued using $H_4[\gamma-H_2SiV_2W_{10}O_{40}] \cdot nH_2O-Ta$ as a catalyst in various reaction time. Figure 7 shows the effect of reaction time to desulfurization of 4-MDBT using $H_4[\gamma-H_2SiV_2W_{10}O_{40}] \cdot nH_2O-Ta$. Reaction time was studied from 1 – 4 h. At the reaction time increase, the conversion of dibenzothiophene was gradually increased until three h to give almost 60% conversion. It can be seen from Figure 7 that at 1 h reaction time, the conversion of dibenzothiophene was 39% and almost similar with reaction at 2 h. Reaction time at four h was slightly decreased from 60% at three h to 49% at four h. Therefore, the optimum oxidation of dibenzothiophene using $H_4[\gamma-H_2SiV_2W_{10}O_{40}] \cdot nH_2O-Ta$ was achieved at 3 h reaction time.

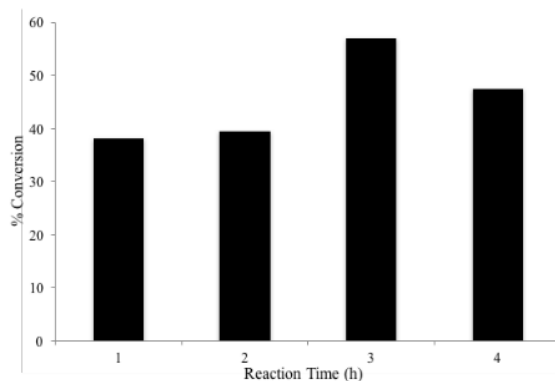


Figure 7. Effect of Reaction Time in the Oxidation of Dibenzothiophene Using $H_4[\gamma-H_2SiV_2W_{10}O_{40}] \cdot nH_2O-Ta$.

3.2.5. Reusability of Catalyst

The $H_4[\gamma-H_2SiV_2W_{10}O_{40}] \cdot nH_2O$ -Ta catalyst can be removed from reaction mixtures due to heterogeneous properties of $H_4[\gamma-H_2SiV_2W_{10}O_{40}] \cdot nH_2O$ -Ta. Catalyst $H_4[\gamma-H_2SiV_2W_{10}O_{40}] \cdot nH_2O$ -Ta was collected from the reaction mixtures by conventional filtration. The catalyst was dried and washed using methanol and water, respectively. Furthermore, the catalyst was dried at 110 °C before use.

Desulfurization of dibenzothiophene using reuse catalyst was conducted using 0.1 g catalyst at 70 °C, for three hours reaction time. The results as shown in Table 2 showed that reuse catalyst was slightly decreased the catalytic activity of $H_4[\gamma-H_2SiV_2W_{10}O_{40}] \cdot nH_2O$ -Ta about 24%. This condition may be attributed to inactivation of several active sites on $H_4[\gamma-H_2SiV_2W_{10}O_{40}] \cdot nH_2O$ -Ta during recovery or oxidation processes.

Table 2. Recycling of Catalyst $H_4[\gamma-H_2SiV_2W_{10}O_{40}] \cdot nH_2O$ -Ta

Recycling Catalyst	% DBT Conversion
Fresh catalyst	60.00
1 st recycle	45.06

4. Conclusion

Supported polyoxometalate $H_4[\gamma-H_2SiV_2W_{10}O_{40}] \cdot nH_2O$ has high crystallinity after impregnation process with bulky structure. Supported polyoxometalate $H_4[\gamma-H_2SiV_2W_{10}O_{40}] \cdot nH_2O$ with metal oxides showed moderate to high catalytic activity with regeneration catalyst ability for first reuse process.

5. References

- [1]. Dincer, I., Zamfirescu, C. 2014. Fossil Fuel and Alternatives: Advanced Power Generation Systems. Chapter 3, 95-141.
- [2]. Zhao, Y., Ma, Q., Liu, Y., He, H. 2016. Influence of Sulfur in Fuel on the Properties of Diffusion Flame Soot. *Atmospheric Environment*. 142, 383-392.
- [3]. Xiao, J., Wu, L., Wu, Y., Liu, B., Dai, L., Li, Z., Xia, Q., Xi, H. 2014. Effect of Gasoline Composition on Oxidative Desulfurization Using a Phosphotungstic Acid/Activated Carbon Catalyst with Hydrogen Peroxide. *Applied Energy*, 113, 78-85.
- [4]. Alvarez-Amparán, M.A., Cedeño-Caero, L. 2017. MoOx-VOx Based Catalysts For the Oxidative Desulfurization of Refractory Compounds: Influence of MoOx-VOx Interaction on the Catalytic Performance. *Catalysis Today*. 282(2), 133-139.
- [5]. García-Gutiérrez, J.C., Laredo, G.C., García-Gutiérrez, P., Jimenez-Cruz, F. 2014. Oxidative Desulfurization of Diesel Using Promising Heterogeneous Tungsten Catalysts and Hydrogen Peroxide. *Fuel*. 138, 118-125.
- [6]. Yan, X-M., Mei, P., Xiong, L., Gao, L., Yang, Q., Gong, L. 2013. Mesoporous Titania-Silica-Polyoxometalate Nanocomposite Materials For Catalytic Oxidation Desulfurization of Fuel Oil. *Catalysis Science & Technology*. 3, 1985-1992.
- [7]. Jalilian, F., Yadollahi, B., Farsani, M.R., Tangestaninejad, S., Rudbari, H.A., Habibi, R. 2015. New Perspective to Keplerate Polyoxomolybdates: Green Oxidation of Sulfides with Hydrogen Peroxide in Water. *Catalysis Communications*. 66, 107-110.
- [8]. Fraile, J.M., Gil, C., Mayoral, J.A., Muel, B., Roldán, L., Vispe, E., Calderón, S., Puente, F. 2016. Heterogeneous Titanium Catalysts For Oxidation of Dibenzothiophene in Hydrocarbon Solutions with Hydrogen peroxide: On the Road to Oxidative Desulfurization. *Appl. Catal. B: Environmental*. 180, 680-686.
- [9]. Zhang, J., Wang, A., Li, X., Ma, X. 2011. Oxidative Desulfurization of Dibenzothiophene and Diesel Over $[Bmim]_3PMO_{12}O_{40}$. *J. Catal.* 279, 269-275.

- [10]. Wang, D., Liu, N., Zhang, J., Zhao, X., Zhang, W., Zhang, M. 2014. Oxidative Desulfurization Using Ordered Mesoporous Silicas as Catalysts. *J. Mol. Catal. A: Chemical*. 393, 47-55.
- [11]. Trehoux, A., Roux, Y., Guillot, R., Mahy, J-P., Avenier, F. 2015. Catalytic Oxidation of Dibenzothiophene and Thioanisole by a Diiron(III)Complex and Hydrogen Peroxide. *J. Mol. Catal. A: Chemical*. 396, 40-46.
- [12]. Long, Z., Yang, C., Zeng, G., Peng, L., Dai, C., He, H. 2014. Catalytic Oxidative Desulfurization of Dibenzothiophene Using Catalyst of Tungsten Supported on Resin D152. *Fuel*. 130, 19-24.
- [13]. Wang, R., Zhang, G., Zhao, H. 2010. Polyoxometalate as Effective Catalyst for the Desulfurization of Diesel Oil. *Catalysis Today*. 149, 117-121.
- [14]. Hill, C.L. 2007. Progress and Challenges in Polyoxometalate-Based Catalysis and Catalytic Materials Chemistry. *J. Mol. Catal. A: Chemical*. 262, 2-6.
- [15]. Sinaga, L., Lesbani, A. 2017. Thermal Stability Effect of $H_4[PVMo_{11}O_{40}]/SiO_2$. *Science and Technology Indonesia*. 2,1, 25-28.
- [16]. Trakarnpruk, W., Rujiraworawut, K. 2009. Oxidative Desulfurization of Gas Oil by Polyoxometalates Catalysts. *Fuel Processing Technology*. 90, 411-414.
- [17]. Torres-García, E., Galano, A., Rodríguez-Gattorno, G. 2011. Oxidative Desulfurization (ODS) of Organosulfur Compounds Catalyzed by Peroxo-metallate Complexes of WO_x-ZrO_2 : Thermochemical, Structural, and Reactivity Indexes Analyses. *J. Catal.* 282, 201-208.
- [18]. Qiu, J., Wang, G., Zhang, Y., Zeng, D., Chen, Y. 2015. Direct Synthesis of Mesoporous $H_3PMo_{12}O_{40}/SiO_2$ and Its Catalytic Performance in Oxidative Desulfurization of Fuel Oil. *Fuel*. 147, 195-202.
- [19]. Rezvani, M.A., Shojaie, A.F., Loghmani, M.H. 2012. Synthesis and Characterization of Novel Nanocomposite, Anatase Sandwich Type Polyoxometalate, as a Reusable and Green Nano Catalyst in Oxidation Desulfurization of Simulated Gas Oil. *Catalysis Communications*. 25, 36-40.
- [20]. Lesbani, A., Marpaung, A., Fithri, N.A., Mohadi, R. 2016. 12-Tungstophosphoric Acid/Silica catalyst for Oxidation of Benzothiophene. *Asian. J. Chem.* 28(3): 617-621.
- [21]. Nakagawa, Y., Mizuno, N. 2007. Mechanism of $[\gamma-H_2SiV_2W_{10}O_{40}]^{4-}$ Catalyzed Epoxidation of Alkanes with Hydrogen Peroxide. *Inorg. Chem.* 46 (5): 1727-1736, doi: 10.1021/ic0623258.
- [22]. Canny, J., Thouvenot, R., Tézé, A., Hervé, G., Leparulo-Loftus, M., Pope, M.T. 1991. Disubstituted Tungstosilicates. 2. γ - and β -Isomers of $[SiV_2W_{10}O_{40}]^{6-}$: Syntheses and Structure Determinations by ^{183}W , ^{51}V , and ^{29}Si NMR Spectroscopy. *Inorg. Chem.* 30(5): 976-981, doi: 10.1021/ic00005a020.
- [23]. Newman, A.D., Brown, D.R., Siril, P., Lee, A.F., Wilson, K. 2006. Structural Studies of High Dispersion $H_3PW_{12}O_{40}/SiO_2$ Solid Acid Catalysts. *Phys. Chem. Chem. Phys.* 8(24): 2893-2902, doi: 10.1039/b603979k.
- [24]. Poźniczek, J., Lubańska, A., Micek-Ilnicka, A., Mucha, D., Lalik, E., Bielański, A. 2006. TiO_2 and SiO_2 Supported Wells-Dawson Heteropolyacid $H_6P_2W_{18}O_{62}$ as the Catalyst for MTBE Formation. *Appl. Catal. A: General*. 298(1):217-224, doi: 10.1016/j.apcata.2005.10.013.
- [25]. Leilei, X., Yihang, G., Huiru, M., Jianguo, G. 2013. Heterogeneous Acid Catalytic Esterification by Porous Polyoxometalate-Tantalum Pentoxide Nanocomposites. *Journal of Wuhan University of Technology-Mater.Sci.Ed.* 28(3):580-585, doi: 10.1007/s11595-013-0734-1.
- [26]. Lesbani, A., Agnes, A., Saragih, R.O., Verawaty, M., Mohadi, R., Zulkifli, H. 2015. Facile Oxidative Desulfurisation of Benzothiophene Using Polyoxometalate $H_4[\alpha-SiW_{12}O_{40}]/Zr$ Catalyst. *Bull. Chem. React. Eng. Catal.* 10(2): 185-191, doi: 10.9767/bcrec.10.2.7734.185-191.
- [27]. Lesbani, A., Gultom, E.O.J. 2017. Synthesis and Characterization of Metal Oxides Supported Keggin Type Polyoxometalate $Rb_2K_2[H_2SiV_2W_{10}O_{40}].nH_2O$. *Science and Technology Indonesia*. 2.2, 50-55.
- [28]. Mohadi, R., Teresia, L., Fithri, N.A., Lesbani, A., Hidayati, N. 2016. Oxidative Desulfurization of Dibenzothiophene Using Dawson Type Heteropoly Compounds/Tantalum as Catalyst. *Indones. J. Chem.* 16(1): 105-110.

6. Acknowledgement

This research is a part of Hibah Profesi 2017. AL thank to Universitas Sriwijaya for “Hibah Profesi 2017” contract number 987/UN9.3.1/PP/2017. Authors thank Integrated Research Laboratory of Graduate School, Sriwijaya University for GC equipment for this experimental research.

C.2a.1.8-

Lesbani_2018_IOP_Conf._Ser._Mater._Sci._Eng._299_01208...

ORIGINALITY REPORT

14%

SIMILARITY INDEX

PRIMARY SOURCES

1	kyutech.repo.nii.ac.jp Internet	144 words — 5%
2	nsm.bstu.ru Internet	68 words — 2%
3	www.semanticscholar.org Internet	46 words — 1%
4	ejournal.undip.ac.id Internet	35 words — 1%
5	kar.kent.ac.uk Internet	29 words — 1%
6	pubs.rsc.org Internet	28 words — 1%
7	oparu.uni-ulm.de Internet	21 words — 1%
8	citeseerx.ist.psu.edu Internet	19 words — 1%
9	www.sersc.org Internet	19 words — 1%

10

worldwidescience.org

Internet

16 words — 1%

EXCLUDE QUOTES OFF

EXCLUDE MATCHES < 1%

EXCLUDE BIBLIOGRAPHY ON